

HIM: A Linear Free-Surface Model for Irrigation Canals Operating in Real Time

E. Bonet^{1*}, M. T. Yubero², P. Alfonso³, J. Soler⁴

¹ Department of Mining, Industrial and ICT Engineering, Universitat Politècnica de Catalunya (UPC), Les Bases Avenue 61-73, 08242 Manresa, Spain. Email: enrique.bonet@upc.edu

² Department of Mining, Industrial and ICT Engineering, Universitat Politècnica de Catalunya (UPC), Les Bases Avenue 61-73, 08242 Manresa, Spain. Email: maria.teresa.yubero@upc.edu

³ Department of Mining, Industrial and ICT Engineering, Universitat Politècnica de Catalunya (UPC), Les Bases Avenue 61-73, 08242 Manresa, Spain. Email: maria.pura.alfonso@upc.edu

⁴ Barcelona School of Civil Engineering, Department of Civil and Environmental Engineering, C/ Jordi Girona, 1,08034 Barcelona, Spain

*Corresponding Author: E. Bonet

ARTICLE INFO

Received: 18 Dec 2024

Revised: 10 Feb 2025

Accepted: 19 Feb 2025

ABSTRACT

One of the most significant contributions in the paper is the concept of the Hydraulic Influence Matrix (HIM) and its use as a linear model for complex open-flow canals. In the context of canal flow, the HIM serves as a parameter sensitivity matrix. Given its physical interpretation, the HIM can characterize free-surface flow behavior in canals. Specifically, it helps analyze the dependence domain of a canal setpoint and the influence domain of a gate movement.

The matrix is populated with derivatives typically calculated using numerical flow models, but this approach is impractical when there are many parameters to identify or when the performance index is challenging to evaluate common issues in canal control systems. Therefore, the HIM has been derived analytically. A primary contribution of the HIM to open-flow canals and canal controllers is its ability to quickly and accurately compute water level and velocity perturbations in response to gate movements in real-time. This model provides watermasters with the ability to apply this linear surface model in both unsteady and steady states, enabling real-time applications in control algorithms. Model testing showed that, for gate movement disturbances ranging between 10% and 0.5%, equivalent to a maximum incremental discharge of over 70%, the linear model maintains an acceptable error margin, supporting its application as a real-time control model. Furthermore, this model fully supports real-time control applications, as larger gate movement disturbances (exceeding 10%) should be planned in advance rather than managed in real time.

Keywords: Optimization algorithms, real time control, mathematical flow models, irrigation canals.

OBJECTIVE

Climate change has a negative impact on the quantity and quality of available water needed to meet global human needs according to UNESCO [1]. The global population is rapidly growing, with expectations of reaching 8 billion people in 2030 and being just shy of 10 billion people in 2050 according to the United Nations [2], both of which are figures that suggest an imminent surge in global food demand. Irrigated agriculture is the most water-intensive sector, consuming around of 60-80% of water resources in a country [3]. Moreover, irrigation water distribution systems are the infrastructure by which one-third of water resource losses take place. Monitoring and controlling operations in irrigation canals are essential for mitigating leakages and water waste in operational actions.

The problem of adjusting the discharges of an irrigation canal to meet demands by farmers at outlets requires a certain ability to control the canal. Once the farmer's demands in a time horizon are known and ordered to

watermaster, it is necessary to define the gate movements along time in the canal so as to provide the required discharge at the required time. This control problem is divided into two steps in [4] and [5]: the off-line feedforward stage (planification stage) and the real-time feedback stage (operational stage). The first step is solved by means of a Feedforward Control Algorithm such as volume compensation algorithms [6] or more sophisticated from nonlinear optimization problem with constraints such as as PILOTE [7], LQR optimal control [8], predictive algorithms such as [9-11] “GoRoSo” in [4] and the second step could be solved by a feedback control algorithm such as “GoRoSoBo” [5].

In this context, the study of the flow transients can be made by means of the complete Saint-Venant equations because they require much time to compute the simulations. But in the context of the Feedback Control that is used in real time, we have not enough time to know the flow prediction based on the complete Saint Venant model. To reduce the computational time for the obtaining of canal flow behavior, the linear model around of an unsteady state is proposed.

The linear model around of an unsteady state is based on the HIM matrix which is able to estimate the influence of any disturbance introduced in the irrigation canal in its behavior, which is a useful to apply with a feedback control to operate canal gates in real time.

METHODOLOGY: THE HYDRAULIC MODEL

Free surface flow equations

The equations of Barré de Saint-Venant (1871) describe the free-surface flow in prismatic canals and are the result of the application of the principles of mass conservation and of the quantity of movement in a controlled volume of short length in the direction of flow. A rigorous deduction of these equations for prismatic canals can be found in [12], resulting in:

$$\left. \begin{aligned} \frac{\partial y}{\partial t} + v \frac{\partial y}{\partial x} + \frac{A(y)}{T(y)} \frac{\partial v}{\partial x} &= 0 \\ \frac{\partial v}{\partial t} + v \frac{\partial v}{\partial x} + g \frac{\partial y}{\partial x} &= g [S_0 - S_f(y, v)] \end{aligned} \right\} \tag{1}$$

Where x and t are the independent space and time variables, y is the level of the free-surface from canal bottom, v is the average velocity of all particles of a cross section of the flow, A(y) is the area of wet section which depends on the depth, T(y) is the maximum width also dependent on the depth, S₀ is the canal bottom slope, and finally, S_f(y, v) is the slope friction. These equations cannot be solved analytically, only numerically. Thus, a variety of numerical methods exist, which can be found, among others, in [13].

Usually, equations (1) are expressed in the classical space and time (x/t) axes, but in case that we use the so called characteristic curves, these equations are represented in two curves or characteristics curves, expressed parametrically with x+(t) (downstream curve) and x-(t) (upstream curve) which locally satisfy the two following differential equations:

$$\left. \begin{aligned} \frac{dx^+}{dt} &= v + c(y) \\ \frac{dx^-}{dt} &= v - c(y) \end{aligned} \right\} \quad \left. \begin{aligned} \frac{dv}{dt} + \frac{g}{c(y)} \frac{dy}{dt} &= g[S_0 - S_f(y, v)] \\ \frac{dv}{dt} - \frac{g}{c(y)} \frac{dy}{dt} &= g[S_0 - S_f(y, v)] \end{aligned} \right\} \quad c(y) = \sqrt{\frac{gA(y)}{T(y)}} \tag{2}$$

The nice effect of the transformation of the method of characteristics is that the partial differential equations (1) become an ordinary differential equation system. The difficulty of the method lies in the fact that the equations (1) have to be solved along the characteristic curves or the local axes that are the solution of (2). As this last one is a set of non-linear equations, it obliges us to solve the four equations simultaneously. Fortunately, the curves x+(t) and x-

(t) always intersect, although they are not orthogonal, and therefore assure hyperbolicity. The system (2) can be represented in the graph x/t as in Figure 1 where, at the point of intersection R , the four equations are satisfied and therefore the four unknowns x , t , y and v can be found theoretically. This way, if flow conditions at points P and Q are known, the position of point R can be found and integrated numerically, along with the flow conditions.

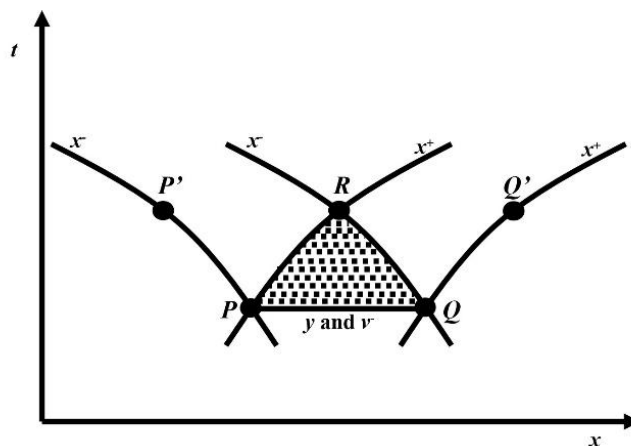


Figure 1: The dependence domain of point R.

The discretization of the characteristic equations

As previously mentioned, the system (1) and the equivalent (2) have no known analytical solution, and therefore, the use of numerical techniques has, until present, been compulsory. In this paper we have preferred to use a specific discretization and make the appropriate mathematical developments based on the result of this discretization. In order to have the longest possible integration time period without loss of precision, we have adopted a discretization in finite differences of second order, called in [14] as "the method of characteristic curves" applying to a structured grid.

In Figure 2, you can see how by placing the characteristic curves net (Figure 2 a)) on top of a structured net (Figure 2 b)) a new scheme is obtained where the variables for points P and Q are interpolated at time step k (Figure 2 c)). In this way we can obtain the flow conditions for the fixed-point R at a time step $k+1$.

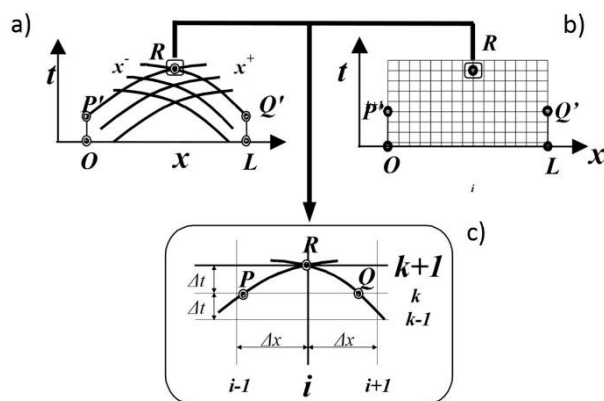


Figure 2: The steps for the interpolation onto a structured grid.

In any case, the irrigation canals are controlled by control structures which are built along the canal, see [15-17]. There are many flow control structures in canals which allow flow modeling according to the specification of the

watermaster. The individual study of each of these structures is impossible in this work and does not fall within its aims. However, we present as an example a commonly found structure. It is a checkpoint with a sluiceway, a lateral weir outlet and a pumping, as seen in Figure 3 (a-b). The interaction of this control structure with the flow can be described according to the principles of mass and energy conservation. These principles establish two mathematical relations between the flow conditions just upstream and downstream of the checkpoint:

$$\left. \begin{aligned} S(y_e) \frac{dy_e}{dt} &= A(y_e)v_e - q_b - q_s(y_e) - A(y_s)v_s - q_{\text{offtake}}(y_e) \\ q_{\text{offtake}}(y_e) &= C_d A_o \sqrt{2gy_e} \\ A(y_s)v_s &= k_c u \sqrt{y_e - y_s + d} \end{aligned} \right\} \quad (3)$$

Where: $S(y_e)$ is the horizontal surface of the reception area in the checkpoint., $A(y_e)v_e$ is the incoming flow to checkpoint, defined in terms of water depth and velocity., $A(y_s)v_s$ is the outgoing flow to checkpoint which continues along the canal, described in terms of water depth and velocity, q_b is the pumping offtake, which is predetermined, $q_s(y_e) = C_s a (y_e - y_0)^{3/2}$ is the outgoing lateral flow via the weir where C_s is the discharge coefficient, a is the width of the lip and y_0 is the height of the lip measured from the bottom, $k_c = \sqrt{2g} C_c a_c$ where C_c is the discharge coefficient of the sluiceway and a_c is the sluiceway width, q_{offtake} is the outgoing offtake orifice flow where C_d is the discharge coefficient, A_o is the area of the offtake orifice, d is the checkpoint drop, u is the sluiceway opening.

The presence of checkpoints, where water level sensors are deployed, in the middle of a canal leads to the sub-division of this canal into canal pools, in a way that there is a canal pool between two checkpoints, and there is a checkpoint between two pools. The checkpoints are located and dorsed in control structures position, see Figure 3 (b). Therefore y_n^{k+1} represents the water level at node n in the section upstream of the control point at time $k+1$, that is to say, the incoming water level y_e (Figure 3 b).

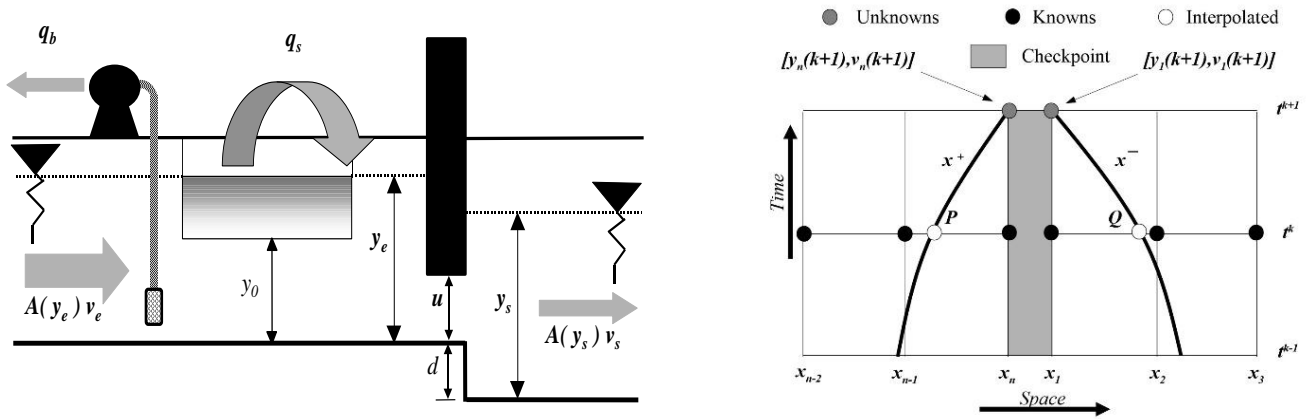


Figure 3a: Diagram of a checkpoint with gate, lateral weir and pumping. Figure 3b: Graph with discretization of checkpoints

If discretization is carried out with time and we rewrite the control structures (3), join them with the characteristics of (2) and then change the nomenclature considering a structured grid, we arrive at the following system of six equations:

$$\left. \begin{aligned}
 f_1 &\equiv x_n - x_p - \frac{1}{2} \Delta t \left[v_n^{k+1} + c_n^{k+1} + v_p + c_p \right] = 0 \\
 f_2 &\equiv \left(v_n^{k+1} - v_p \right) + \frac{g}{2} \frac{c_n^{k+1} + c_p}{c_n^{k+1} c_p} \left(y_n^{k+1} - y_p \right) - g \Delta t \left(\frac{S_{f_n}^{k+1} + S_{f_p}}{2} - S_0 \right) = 0 \\
 f_3 &\equiv \left(v_1^{k+1} - v_Q \right) - \frac{g}{2} \frac{c_1^{k+1} + c_Q}{c_1^{k+1} c_Q} \left(y_1^{k+1} - y_Q \right) - g \Delta t \left(\frac{S_{f_1}^{k+1} + S_{f_Q}}{2} - S_0 \right) = 0 \\
 f_4 &\equiv x_1^{k+1} - x_Q - \frac{1}{2} \Delta t \left[v_1^{k+1} - c_1^{k+1} + v_Q - c_Q \right] = 0 \\
 f_5 &\equiv A \left(y_n^{k+1} \right) v_n^{k+1} - q_b - q_s \left(y_n^{k+1} \right) - A \left(y_1^{k+1} \right) v_1^{k+1} - q_{\text{offtake}} \left(y_n^{k+1} \right) = 0 \\
 f_6 &\equiv A \left(y_1^{k+1} \right) v_1^{k+1} - k_c u \sqrt{y_n^{k+1} - y_1^{k+1} + d} = 0
 \end{aligned} \right\} \tag{4}$$

Where: $\Delta t = t^{k+1} - t^k = t^{k+1} - t_Q$, $y_P(x_P) = s(x_P, y_{n-2}^k, y_{n-1}^k, y_n^k)$, $y_Q(x_Q) = s(x_Q, y_1^k, y_2^k, y_3^k)$, $v_P(x_P) = s(x_P, v_{n-2}^k, v_{n-1}^k, v_n^k)$, $v_Q(x_Q) = s(x_Q, v_1^k, v_2^k, v_3^k)$, $c_n^{k+1} = c(y_n^{k+1})$, $c_1^{k+1} = c(y_1^{k+1})$, $S_{f_n}^{k+1} = S_f(y_n^{k+1}, v_n^{k+1})$ and $S_{f_1}^{k+1} = S_f(y_1^{k+1}, v_1^{k+1})$.

Where the unknowns are x_P , y_n^{k+1} , v_n^{k+1} , y_1^{k+1} , v_1^{k+1} and x_Q . In order to continue with the calculation of the influences of a general parameter ϕ , it is necessary to assume that this parameter defines the opening of the gate, this is $u(\phi)$. Therefore, applying once more the implicit function theorem to (4), with the assumption that y_{i-1}^k , v_{i-1}^k , y_i^k , v_i^k , y_{i+1}^k , v_{i+1}^k , y_{i+1}^{k+1} and v_{i+1}^{k+1} now depend on a general parameter ϕ , we can rebuild the equation systems (4) and obtain the next expression:

$$M \frac{\partial}{\partial u(\phi)} \begin{pmatrix} x_P \\ y_1^{k+1} \\ v_1^{k+1} \\ y_n^{k+1} \\ v_n^{k+1} \\ x_Q \end{pmatrix} = N S \frac{\partial}{\partial \phi} \begin{pmatrix} y_{n-2}^k \\ v_{n-2}^k \\ y_{n-1}^k \\ v_{n-1}^k \\ y_n^k \\ v_n^k \\ y_1^k \\ v_1^k \\ y_2^k \\ v_2^k \\ y_3^k \\ v_3^k \end{pmatrix} + L \frac{\partial u}{\partial \phi} \tag{5}$$

Where:

$$\begin{aligned}
 \mathbf{M} &= \frac{\partial(f_1, f_2, f_3, f_4, f_5, f_6)}{\partial(x_p, y_n^{k+1}, v_n^{k+1}, y_1^{k+1}, v_1^{k+1}, x_Q)} \\
 \mathbf{N} &= -\frac{\partial(f_1, f_2, f_3, f_4, f_5, f_6)}{\partial(x_p, y_p, v_p, y_Q, v_Q, x_Q)} \\
 \mathbf{L} &= \left(0 \quad 0 \quad 0 \quad 0 \quad 0 \quad \frac{\partial f}{\partial u} \right)^T \\
 \mathbf{S} &= \frac{\partial(x_p, y_p, v_p, y_Q, v_Q, x_Q)}{\partial(x_p, y_{n-2}^k, v_{n-2}^k, y_{n-1}^k, v_{n-1}^k, y_n^k, v_n^k, y_1^k, v_1^k, y_2^k, v_2^k, y_3^k, v_3^k, x_Q)}
 \end{aligned}$$

The control variable (φ) could be the gate trajectory or pump flow trajectory, that is, another operating variable according to [18-19]. In (5) for the first time, it appears the gate opening $u(\varphi)$ explicitly in the description. These system (5) shows the influence of the parameter φ on flow conditions at time $k+1$ is: the sum of the indirect influence of the conditions at instant k , and the direct influence of the opening at instant $k+1$ through the term $\partial u / \partial \varphi_n^{k+1}$.

THE LINEAR HYDRAULIC MODEL FOR AN IRRIGATION CANAL

If all the matrix files (4) of all the state variables (water level “ y ” and velocity “ v ”) of any j -gate trajectory ($\frac{\partial x}{\partial u}$) are organized and lumped together in a single matrix. The following Hydraulic Influence Matrix denoted by HIM $X(U)$ is obtained which defines the behavior of the irrigation canal (y and v) in every section regarding control operation variables (u):

$$\begin{aligned}
 \mathbf{HIM}_X(U) &= \left[\frac{\partial \mathbf{X}_1^{k_F}(U)}{\partial u_j(1)} \quad \dots \quad \frac{\partial \mathbf{X}_1^{k_F}(U)}{\partial u_j(K)} \quad \dots \quad \frac{\partial \mathbf{X}_1^{k_F}(U)}{\partial u_j(K_F)} \right] = \\
 &= \begin{bmatrix} \frac{\partial \mathbf{x}^1(U)}{\partial u_j(1)} & & \dots & & \frac{\partial \mathbf{x}^1(U)}{\partial u_j(K_F)} \\ & \ddots & & & \vdots \\ \vdots & & \frac{\partial \mathbf{x}^k(U)}{\partial u_j(K)} & & \vdots \\ & \ddots & & \ddots & \\ \frac{\partial \mathbf{x}^{k_F}(U)}{\partial u_j(1)} & & \dots & & \frac{\partial \mathbf{x}^{k_F}(U)}{\partial u_j(K_F)} \end{bmatrix} \tag{6}
 \end{aligned}$$

RESULTS: VERIFICATION OF THE LINEAR HYDRAULIC MODEL

In order to show the accuracy of our Linear Model V.S. a model using the Saint Venant in their complete form, we will be evaluate the both model taking account a disturbance introduced in a canal on steady state. This test is done in an illustrative example. We can further illustrate the concept of the influence of a gate trajectory variable on the state vector. To do this, consider a numerical example based on a simulation carried out on a 5 Km long canal with two pools and three checkpoints, see Figure 4 and Table 1. Each pool is divided in 125 numerical cells and therefore there are 126 computational nodes and $n_S = n_I + n_{II} = 126 + 126 = 252$ (cross sections). In this manner, the state vector has 504 components. The boundary conditions are steady, the upstream boundary conditions (checkpoint 0) is a constant water level H and the downstream boundary condition (outlet) is a particular discharge Q (checkpoint 2). In order to achieve this steady state-vector, the gate-position trajectory also has to be steady in the time period of simulation. The features of the canal are shown in the next tables:

Table 1: Canal features.

Pool number	Pool length (Km)	Bottom slope (%)	Side slopes (H:V)	Manning’s coefficient (n)	Bottom width (m)	Canal Depth (m)
I	2.5	0.1	1.5:1	0.025	5	2.5
II	2.5	0.1	1.5:1	0.025	5	2.5

Table 2: Sluice gates features (canal structures).

Gate discharge coefficient	Gate width (m)	Gate height (m)	Step (m)
0.61	5.0	2.0	0.6
0.61	5.0	2.0	0.6

Table 3: Pump station/ orifice offtake features (canal structures).

Number of control structure or checkpoint	Discharge coef./ diameter orifice offtake (m)	Orifice offtake height (m)	Pump flow (m ³ /s)
0*	-	-	-
1	2/0.85	0.8	-
2	-	-	5.0

Table 4: Initial conditions in the canal.

Control structure	Initial Flow rate (m ³ /s)	Control structure	Initial water level upstream (m)/ offtake orifice outflow (m ³ /s)	Control structure	Pump flow discharge (m ³ /s)
Gate 0	10.0	Checkpoint 1	2.0/5.0	Checkpoint 2	5.0

In these examples are considered an upstream large reservoir, whose water level $H_{\text{reservoir}}$ is 3 m constant throughout the test. At the middle of the canal (end of the pool 1), there is a control structure (checkpoint 1) with a gate and an orifice offtake (7), see Table 2 and 3, which discharge 5 m³/s.

$$q_{\text{offtake}} = C_d A_0 \sqrt{2g(y - y_0)} \tag{7}$$

Where C_d is the discharge coefficient for an offtake orifice, A_0 is the area of the offtake orifice where y is the water level in canal at offtake, y_0 is the orifice offtake height. At the end of the last pool, there is a control structure with a pump station, which discharge 5 m³/s. The flow through the orifice depends on the level over the orifice and the disturbance. This example starts from an initial steady state (Table 4) with a specific demand delivery constant at the checkpoint 1 (5m³/s through the orifice offtake), and a constant discharge of 5 m³/s by the pump station at checkpoint 2. The disturbance is not introduced initially.

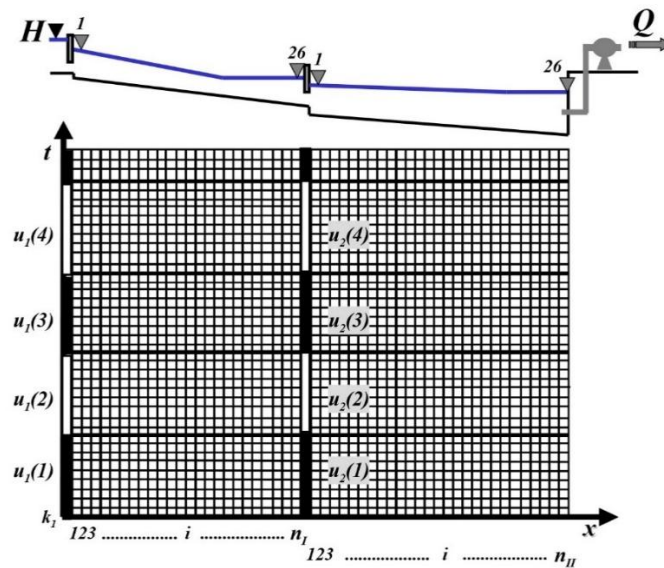


Figure 4: Sketch of the numerical example based on canal with two pools and two checkpoints. It is shown the water depth profile with H as the upstream water level and Q as the downstream discharge.

At checkpoint 0 and 1, there is a gate, which is operated according to the watermaster from initial conditions, see Table 2 and 4. The error among both models (linear hydraulic model VS Saint Venant in complete form) is estimated from absolute error and maximum relative error.

Absolute error or I_1 (cm)

Maximum relative error or I_2 (%)

$$Max(y_{pi} - y_i) \tag{8}$$

$$Max\left(\sum_{i \geq 1}^n \left(\frac{y_{pi} - y_i}{y_i}\right) \times 100\right) \tag{9}$$

Where y_{pi} is the water level obtained by the linear model at the instant i at a checkpoint, y_i is the water level obtained by the Saint Venant complete form at the instant i at a checkpoint, n is number of time step, the value of time step is 300 seconds for the test over 4 hours.

These indexes (I_1 and I_2) give us an idea how far the linear solution is to the Saint Venant in their complete form. The way to set the gate-movement it is from, a maximum flow disturbance assumed for the system on a context of a feedback control (Table 5). In other words, the criteria is the maximum perturbation admitted working in real time.

For that reason, it would be useful show the initial and the perturbed discharge under the sluice gate number two.

$$Q = C_d BA \sqrt{2g(\Delta H)} \tag{10}$$

Where, Q is the flow discharge sluice gate, C_d is the discharge coefficient for a gate, B is the width-gate, A is the gate opening, and ΔH is the height difference between the headwater depth and the tailwater depth.

The flow discharge by the gate 1 (checkpoint 1) is $5 \text{ m}^3/\text{s}$ in a steady state, and the flow discharge introducing by a gate movement of 10% over the gate height is $8.57 \text{ m}^3/\text{s}$. In other words, this gate movement involve an incremental discharge more than 70 %. For that reason, introduce a gate-movement higher 10% is not the target of this paper, due to the fact that the HIM simulated lineal model is used in real time, and this sort of disturbance is quite difficult to manage in real time, just by feedforward controls. As a conclusion, the gate movement disturbance would be established between 10% and 0.5%.

In that test is performed four cases, nevertheless the position of the disturbance in time is always the same (the range step from 300s to 600s). The differences between cases depends on the value of the disturbance.

Table 5: Disturbance value set in the cases

	Case1	Case2	Case3	Case4
$\Delta U_2(2)$	25 cm (10%)	12.5 cm (5%)	2.5 cm (1%)	1.25cm (0.5%)

Table 6: Index error between Linear Hydraulic Model and the Saint-Venant in their complete form

	I ₁ (cm)		I ₂ (%)	
	Checkpoint 0	Checkpoint 1	Checkpoint 0	Checkpoint 1
Case 1	4,1	6,8	0,17	0,65
Case 2	0,9	3,5	0,03	0,33
Case 3	0,1	0,7	0	0,06
Case 4	0	0,4	0	0,03

The results obtained in the four cases are shown in Table 6, we can see that the error of the first index is only important in case 1 which the disturbance is 70% over the flow canal, and the values for second index are not such important. To remark, the HIM (linear model) is a great model to know the flow behaviour in real time, where the flow disturbance are little and you need to know the simulated flow state quickly and accurate.

CONCLUSIONS

The procedure showed in this paper is summarized in the following: starting from the Saint-Venant model and the checkpoint equations, a set of numerical equations has been established by the method of characteristics. Taking the resulting system of algebraic equations as a base and using the implicit function theorem, the procedure obtains the derivatives of the flow conditions respect to the gate-parameters and all of them are joined into the HIM.

The HIM can be used as a linealization of the Saint-Venant model to build a linear hydraulic model in the context of real-time optimal control to reduce the computation time, in order to known the canal flow behavior. As result, due to the little difference of the simulated free surface between both models considering low disturbances. We reach at the conclusion that the linear model can be used as predictive model of the canal state in real time. In conclusion, for gate movement disturbances ranging between 10% and 0.5% equivalent to a maximum incremental discharge of over 70% the linear model demonstrates an acceptable error margin for application as a real-time control model.

REFERENCES

[1] Alizadeh, M.R.; Ehsani, A.H.; Omid, M.; Makui, A. Optimal operation of pumping stations in irrigation networks. *J. Irrig. Drain.Eng.* 2003, 129, 104–112.3. Bohórqueza, J.; Saldarriaga, J.;

[2] Vallejoa, D. Pumping pattern optimization in order to reduce WDS operation costs. In *Proceed-ings of the 13th Computer Control for Water Industry Conference, CCWI 2015, Leicester, UK.* <https://doi.org/10.1016/j.pro-eng.2015.08.936>. (2 Sept 2015 - 4 Sept 2015).

[3] Ingrao, C., Strippoli, R., Lagioia, G., & Huisingh, D. (2023). Water scarcity in agriculture: An overview of causes, impacts and approaches for reducing the risks. *Heliyon*, 9(8), e18507. <https://doi.org/10.1016/j.heliyon.2023.e18507>

[4] Soler, J., Gómez, M., Rodellar, J., (2008), “A control tool for irrigation canals with scheduled demands”, *Journal of Hydraulic Research*, Vol. 46, Extra Issue, pp. 152-167.

[5] Bonet E., Gómez, M., Yubero, M. T., Fernández-Francos, J., 2017. GOROSOBO: an overall control diagram to improve the efficiency of water transport systems in real time. *Journal of Hydroinformatics*. Available Online: 2017 Mar, jh2017225; DOI: 10.2166/hydro.2017.225.

- [6] Liao, W.; Guan, G.; Tian, X. Exploring Explicit Delay Time for Volume Compensation in Feedforward Control of Canal Systems. *Water* 2019, *11*, 1080. <https://doi.org/10.3390/w11051080>
- [7] Malaterre P.O. (1995), "PILOTE: optimal control of irrigation canals", First International Conference on Water Resources Engineering, Irrigation and Drainage, San Antonio, Texas, USA.
- [8] Malaterre, P.O., (1994), "Modelisation, Analysis and LQR Optimal Control of an Irrigation Canal", PhD Thesis LAAS-CNRS-ENGREF-Cemagref, Etude EEE n°14, ISBN 2-85362-368-8, FR.
- [9] Gómez, M., Rodellar, J. and Mantecón, J. (2001), "Predictive control method for decentralized operation of irrigation canals", *Applied Mathematical Modelling Journal*, Vol 26, pp.1039-1056.
- [10] Rodellar, J., Gómez, M., Martín, J.P., (1989) "Stable Predictive Control of Open-Channel Flow", *Journal of Irrigation and Drainage Engineering*, Vol 115.
- [11] Gejadze, I., Malaterre, P. O., (2016). Discharge estimation under uncertainty using variational methods with application to the full Saint-Venant hydraulic network model. *Int. J. Numer. Meth. Fluids* (2016); DOI: 10.1002/flid.4273.
- [12] Walker, W.R., Skogerboe, G.V., (1987), *Surface Irrigation. Theory and Practice*, Prentice-Hall, Inc. Englewood Cliffs, New Jersey, US.
- [13] Wylie, 1969, "Control of transient free-surface flow", *Jour. of the Hydr. Div., (ASCE)*, p 347-361. 40.
- [14] Gómez, M., (1988), *Contribución al estudio del movimiento variable en lámina libre, en las redes de alcantarillado. Aplicaciones*, Doctoral thesis UPC, Barcelona. Vol 26, pp.1039-1056.
- [15] Ames, W.F., (1977), *Numerical Methods for Partial Differential Equations*, Academic Press Inc., Orlando, Florida, US.
- [16] Ducheteau, P., Zachmann, D.W., (1988), *Ecuaciones diferenciales parciales*, Ed. McGraw-Hill, Mèxic.
- [17] Crandall. S.H., (1956), *Engineering Analysis-A Survey of Numerical Procedures*, Wiley (Interscience), New York, US.
- [18] Bonet E., 2015. Experimental design and verification of a centralized controller for irrigation canals. PhD. UPC, Technical University of Catalonia.
- [19] Soler, J., Gómez, M., & Bonet, E. (2016). Canal monitoring algorithm. *Journal of Irrigation and Drainage Engineering*, 142(3), 04015058. [https://doi.org/10.1061/\(ASCE\)IR.1943-4774.0000982](https://doi.org/10.1061/(ASCE)IR.1943-4774.0000982).